JOURNAL OF COMPUTATIONAL PHYSICS 67, 279–289 (1986)

Monte Carlo Technique for Simulating the Evolution of an Assembly of Particles Increasing in Number

E. E. KUNHARDT

Polytechnic Institute of New York,
Route 110, Farmingdale, New York 11735

AND

Y. TZENG

Auburn University, Auburn, Alabama 36840

Received March 25, 1985; revised November 1, 1985

We describe an algorithm for simulating the evolution of an assembly of particles which is increasing in number. It is based on the use of the Monte Carlo method and a renormalization procedure which allows the mapping of the growing assembly into another consisting of fewer particles. The results of test calculations are presented and error analysis of the results are included.

I. INTRODUCTION

The average-kinetic description of the evolution of an initial number of particles interacting via binary collisions with a background medium (and/or among themselves) is given by the time dependent distribution of particles in phase-space, $f(\mathbf{v}, \mathbf{r}, t)$. In general, the particles may be under the influence of external fields. The phase-space distribution can, in principle, be obtained from a kinetic equation of the Boltzmann type [1, 2] or from Monte Carlo simulation [3, 4]. At present, the Monte Carlo approach has a number of advantages over the kinetic equation approach: it is relatively easy to implement a 6-dimensional phase-space simulation; it can be easily modified to accomodate any number of particle-background interactions; and it provides considerable physical insight into the evolution of the particle assembly, including fluctuation phenomena.

In the Monte Carlo approach, the dynamical evolution of a small number of particles (from one to a few thousand)) is simulated. These particles are representative of the system under investigation. The accuracy of the results depends on the number of particles used in the simulation [5]. A major drawback of this approach is that the simulation takes a considerable amount of time, even when very few particles are used. The simulation time becomes particularly prohibitive when the num-

0021-9991/86 $3.00

ber of particles in the system increases with time, through interactions with the background. Normally, the particles being generated are neglected in a simulation, so that the total number stays constant. This procedure is not suitable if the effect of the new particles on the total distribution is sought, and if the dynamics of the evolution depends on the total number and distribution of the particles. An example of this situation is the space-time evolution of an initial number of electrons immersed in a background gas of atoms–molecules and influenced by external and space-charge fields. In this case, ionization of the background gas by electron impact rapidly increases the total number of electrons (an electron avalanche). The evolution of the electron assembly is affected by the space-charge fields generated by the growing electron and ion populations. To determine the space-charge field, a knowledge of the total population is necessary.

We have developed a Monte Carlo technique that can be used to simulate the evolution of an assembly of particles growing in number. We have applied the technique to the simulation of the avalanche growth of an initial number of electrons to very large numbers. From the simulation, the phase-space distribution of the growing assembly has been determined. Moreover, with our technique we can investigate regions of the distribution where the visitation frequency is low, such as the high energy tail. Poor statistics in this region have been a limitation when a small number of particles have been used.

The Monte Carlo technique is described in the next section. This technique can be applied to any system of particles growing in number, and interacting via binary collisions with a background medium. To illustrate the capabilities of the procedure, in Section III results are presented from simulations of an electron avalanche in nitrogen. An error analysis is also given in this section. Concluding remarks are given in Section IV.

II. The Monte Carlo Technique

Initially, the phase-space distribution of the system of particles under investigation is specified. An initial number of test-particles are then selected that are representative of the initial distribution. That is, test-particles are selected at random, whose position and velocity are determined from the given phase-space distribution. The total number of test-particles may equal the actual number of particles in the system if the simulation time for this number of test-particles is not prohibitively large. For example, in a VAX–780 computer the simulation time for more than 8000 test-particles becomes excessive. If the number of test-particles is taken to be less than the actual number, a "weight" is assigned to each test-particle. The sum of weights over all test-particles equals the total number of particles. The procedure for assigning weights is discussed below.

The simulation of the evolution of the system of test-particles is broken up into time sections of length t_s. The test-particles present at the beginning of a time section are denoted as "primary" test-particles. The properties (position $\mathbf{r}$, and

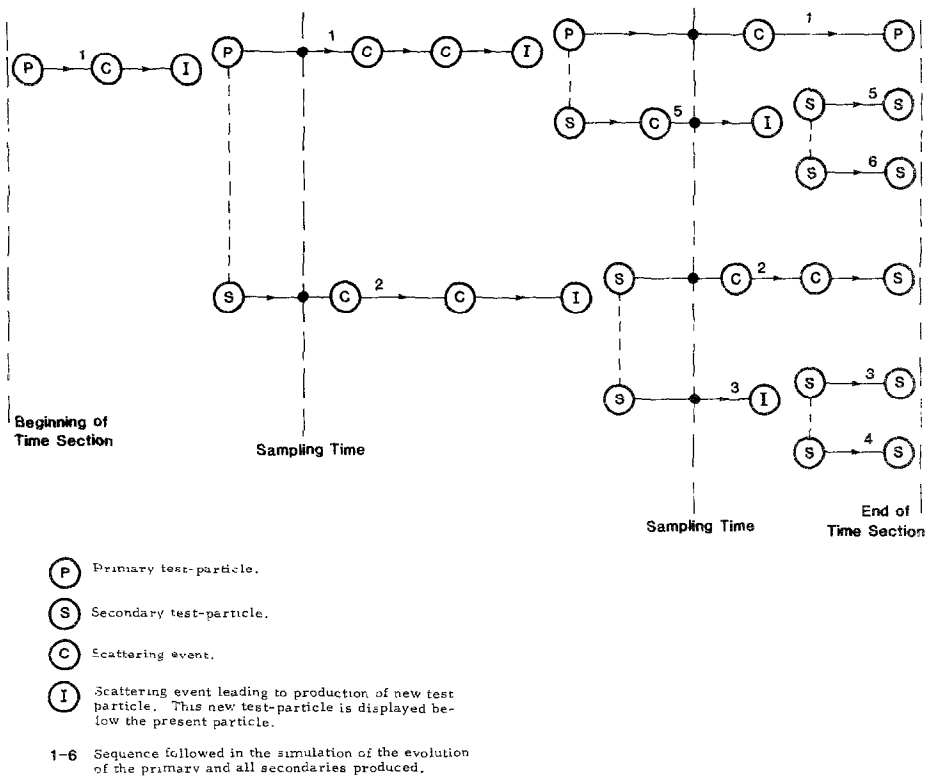

FIG. 1. Sequence followed in tracking all test-particles created by the passage of one "primary" test-particle. This procedure is sequentially applied to all primaries.

velocity **v**) of each of these "primary" test-particles are updated to the end of a time section (how this is done is discussed below). The properties of secondary test-particles that may have been created by the passage of a primary are also updated to the end of the same time section. This is done for all secondaries originating from one primary (including secondaries produced by the passage of other secondaries) before going on to the next primary. This is illustrated in Fig. 1. After all primaries (and the secondaries created by them) have been tracked to the end of a time section, a new one begins with all test-particles present at the end of the previous section as "initial" test-particles. This procedure is repeated in each section until the desired final time, a multiple of t_s.

Since the position and velocity of each test-particle are known at any time, the assembly is completely characterized. In each time section, all desired information about the system can be calculated. The fluctuation in each quantity (i.e., variation from section to section) can also be computed. More will be said about the sampling of information in the next section where an example is discussed.

Updating the Properties of the Test-Particles

The trajectory of a test-particle in phase-space consists of a number of free flights and scattering events. It is assumed that the test-particles obey classical equations of motion during their free flights. That is, between scattering events the position and velocity of a test-particle is determined from the equations:

$$\frac{d\mathbf{r}_i}{dt}(t) = \mathbf{v}_i(t), \qquad \frac{d\mathbf{v}_i}{dt}(t) = \frac{\mathbf{F}_i}{M_i}, \tag{1}$$

where $r_i(t)$, $v_i(t)$, and M_i are the position, velocity, and mass, respectively, of the ith test-particle, and $\mathbf{F}_i$ is the force on it. $\mathbf{F}_i$ may be position and time dependent. The initial conditions for Eqs. (1) are the position and velocity of the test-particle immediately after the last scattering event.

To determine the length of a free path (or the time between scattering events), we have used the "null collision" or "self-scattering" technique [6, 7, 8, 9]. In this technique, the time between scattering events is determined from the equation

$$t_c = [1/Q_c N] \ln[1/(1 - R_1)], \tag{2}$$

where R_1 is a uniformly distributed random number in the interval [0, 1], N is the density of target (background) particles, and Q_c is greater than or equal to the minimum constant that makes $Q_{\text{null}}(v)$ positive for all v in the expression

$$Q_T^1(v) = Q_c v^{-1} = Q_T(v) + Q_{\text{null}}(v). \tag{3}$$

$Q_{\text{null}}(v)$ is the cross section for a fictitious process (null process) which causes no changes in the properties of the test-particle; Q_T is the total cross-section for test-particle-background scattering (assumed to be speed dependent); and Q_T^1 is the effective total cross section after introduction of the null process. Note that Q_T^1 is proportional to v^{-1}.

Although this approach increases the frequency of scattering (since $Q_T^1 > Q_T$), the time between scattering events is much easier to compute (via Eq. (2)) and helps reduce the overall computing time. The alternative [4, 10] would be to compute t_c from the expression

$$R_1 = 1 - \exp\left[-\int_0^{t_c} N Q_T(v(t))\, v(t)\, dt \right]; \tag{4}$$

$v(t)$ in the above equation is obtained from Eq. (1).

Once the length of a free path has been determined (Eq. (2)), the velocity and position of a test-particle can be advanced according to Eq. (1) to the end of the free path. At this time, the test-particle undergoes a scattering event. Let $p_i(v)$ be the probability for the occurrence of the ith scattering process, where

$$p_i(v) = \frac{Q_i(v)}{Q_T^1},$$

Q_i is the total collision cross-section for the ith process (including the null process), and Q_T^1 is defined by Eq. (3). Note that

$$\sum_{i=1}^{n} p_i(v) = 1,$$

where n is the total number of processes including the null process. The type of scattering event that has occurred is determined using a uniformly distributed random number R_2 (in the interval [0, 1]) and the transformation,

$$R_2 = \sum_{i=1}^{j-1} p_i + Sp_j \tag{5}$$

where $0 < S \leqslant 1$. For a given random number R_2, the jth process that satisfies Eq. (5) is assumed to have occurred. The properties of the test-particle are modified according to the process. Subsequently, the time to the next scattering event is determined from Eq. (2), and the whole procedure is repeated.

Mapping the Particle Assembly

A problem encountered in all Monte Carlo calculation is that the number of test particles used in the simulations must be small, if the computation times are not to be prohibitive. This limits the techniques to systems where the number of particles do not grow. To circumvent this limitation, we have developed a renormalization and weighting procedure which maps the test-particle assembly into another consisting of fewer test-particles. This mapping is done to keep equivalent energy distributions between the assemblies and maximum resolution in the high energy tail.

The first mapping occurs at the end of the time section for which the total number of test-particles exceeds a predetermined value, N_t (usually 8000). The equivalent assembly consists of a predetermined fewer number of test-particles, N_i (usually 5,000); where each test-particle may be representative of more than one real-particle, with the number being determined from their weight. Thus, each test-particle is defined by its velocity, position, and weight. When an event occurs where a new test-particle is created, the same weight as the parent is assigned to it. The mapping is subsequently done at the end of each time section for whicht the total number of test-particles exceeds the predetermined value, N_t (i.e., 8000). The length of each time section is adjusted so that the population in the section does not grow by more than the difference between N_t and N_i.

The low frequency of visitation of the test-particles to the high energy tail of the distribution limits the information which can be extracted about the assembly in this region. This is particularly so if a small number of test-particles is used in the simulation or if the mapping mentioned in the previous section is done uniformly. To maintain the statistical information on the high energy tail commensurate with the effective number of test-particles forming the assembly at the time of the mapping, the energy distribution is divided into three sections, and each is mapped

using different factors for the test-particle-to-particle ratio; i.e., the test-particle weights.

The procedure is carried out as follows: first, the test-particles representing all the particles in the assembly are sorted in order of decreasing energy. Second, the total number of test-particles before renormalization, N_t (usually 8,000 by the end of the time section), is partitioned into three groups. Let N_1, N_2, and N_3 correspond to the number of test particles in the three groups with energies in the range $0 \leqslant \varepsilon \leqslant \varepsilon_1$, $\varepsilon_1 < \varepsilon \leqslant \varepsilon_2$, and $\varepsilon > \varepsilon_2$, respectively. ε is the energy of a particle. The mapping is accomplished by using T_1, T_2, T_3 new-test-particles with weights W_1, W_2, W_3, respectively, to represent the N_1, N_2, N_3 group of "old" test-particles, respectively. That is,

$$N_1 = W_1 T_1, \qquad N_2 = W_2 T_2, \qquad N_3 = T_3 W_3,$$

and

$$N_t = N_1 + N_2 + N_3$$

with W_i $(i = 1, 2, 3)$ and T_i $(i = 1, 2, 3)$ chosen, we can find N_i $(i = 1, 2, 3)$ and ε_i $i = 1, 2)$. Typically, the sets (W_1, W_2, W_3) and (T_1, T_2, T_3) are chosen to be (1.8, 1.6, 1.2) and (2000, 2000, 1000), respectively. If we denote the weight of the jth "old" test-particles by W_j' (relative to the actual number of particles), its new weight relative to the actual number of particles is $W_j'' = W_j' W_i$, where $i = 1, 2$, or 3, depending on the group it belongs to after the mapping has been carried out.

Finally, the last X_3 test-particles with the highest energy among the set of N_3 are mapped 1:1. X_3 is typically 100–200 test-particles. The rest of the $N_3 - X_3$ old-test-particles are then mapped onto the remaining $T_3 - X_3$ new-test-particles. The number of "old" test-particles being represented by these $T_3 - X_3$ test-particles is calculated and used as their new weight factor.

This procedure in effect "enhances" the statistics of the high energy tail in that the visitation frequency is equivalent to that obtained with the effective assembly while allowing to follow a smaller number of test-particles. Note that to track the effective assembly would be prohibitively expensive. The validity of the procedure has been confirmed by the fact that when the assembly reaches an equilibrium state (see Sect. IV), fluctuations in transport and rate coefficients due to the mapping are not observed.

III. Example: An Electron Avalanche

The example used to illustrate the technique discussed in the previous section is that of determining the spatio-temporal evolution of a pulse of electrons released from the cathode of a gas filled chamber and subsequently influenced by a uniform applied electric field [11, 12]. A complete ensemble averaged description of the evolution of the electron pulse is in terms of the time-dependent phase-space dis-

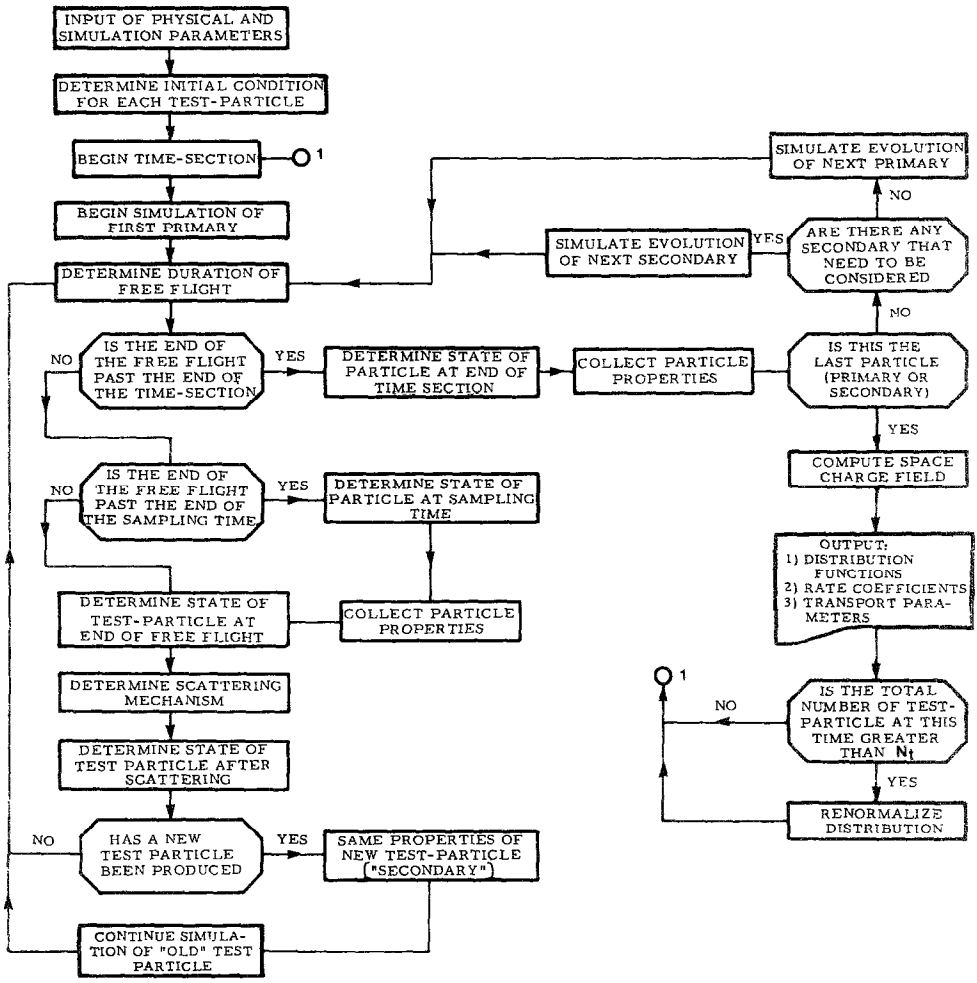

FIG. 2. Flow chart for code used in simulating the evolution of an electron avalanche.

tribution for the population of the various species of particles (electrons, ions, and neutral particles). For the time scales of interest here (nanoseconds), it is only necessary to follow the dynamics of the electrons, i.e., ions and neutrals are assumed stationary. The long range coulomb interactions between the charged species have been taken into account via a space-charge electric field. This field is obtained by solving the Poisson equation, assuming cylindrical symmetry, with the electron and ion densities as the source. The Poisson algorithm has been discussed in detail elsewhere [13]. A flow chart of the code we have developed is shown in Fig. 2. In the example, nitrogen was used as background gas. The total cross-sections for the electron–N_2 reactions used in the simulations have been obtained from

a number of sources [11]. In the case of an ionizing collision, the energy of the secondary is assigned according to the distribution determined from experiments by Opal, Peterson, and Beaty [14].

The initial number of electrons, N_0, released from the cathode ranged from 1 to 1000. For these cases, the initial number of test-particles is equal to the actual number of particles. The initial pulse has a delta function distribution in space, time, and energy. The delta function in energy is at 1 eV. The test-particles leave the cathode at random angles towards the anode. The properties of the initial pulse are an idealization of what would be expected in experiments where a focused, picosecond laser is used to photo-electrically release electrons from the cathode.

As the electrons (test-particles) emerge from the cathode, they accelerate towards the anode, i.e., they gain energy from the field. The electric field to density ratio (E/N) used in the example is 3×10^{-15}V cm^2 (300 Td). The evolution of each electron is computed as discussed in the previous section.

In each time section, all desired quantities are calculated. The maximum length of a time section, t_s is determined by the condition that the assembly does not grow by more than 3000 particles ($N_t - N_i$); that is, there are approximately 3000 ionizing collisions in a time section. At 300 Td, t_s is typically chosen to vary from 0.5 psec for the early stages of development, to 25 psec, for the equilibrium phase. The background density of nitrogen in all simulations is 1×10^{19} cm^{-3}.

To compute the space-averaged energy distribution, $F(\varepsilon)$, the particles are sampled twice during the time section and once at the end of the section. An averaged distribution over the section is thus obtained. The value of t_s used determines the "coarseness" of the distribution in time. Two different widths have been used for the energy bins in computing the distribution; namely, 0,2 eV and 3 eV. The distributions for the smallest bin widths contained 500 points. An example of the distribution obtained is shown in Fig. 3 where the energy distribution, $F(\varepsilon)$, is plotted.

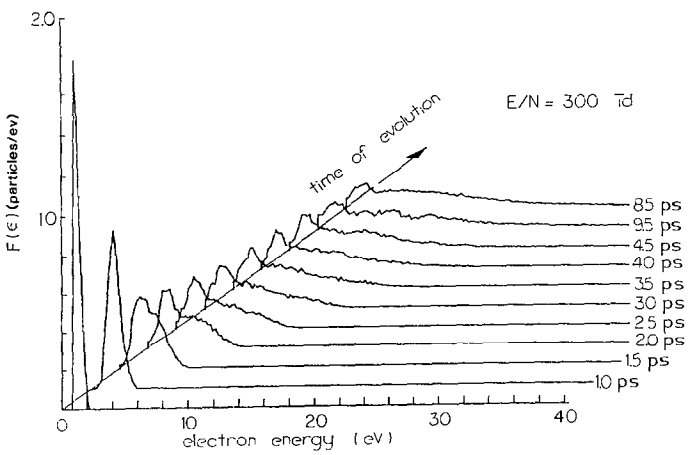

FIG. 3. Evolution of the electron energy distribution, $F(\varepsilon)$.

This "averaged" energy distribution is used in the calculation of the rate coefficients at each time section. In steady state, the maximum fluctuation observed in the ionization rate, ν_i/N, calculated from the distribution at 300 Td is 15%. The large error at 300 Td is due to the few particles that are being sampled at this values of E/N. The error in the other coefficients decreases (to a few percent) since the number of particles sampled increases with decreasing energy treshold for a given process.

The mean electron energy, $\langle \varepsilon \rangle$, is computed by sampling the electron population at the end of each time section. In steady state, the fluctuation in the mean energy has been calculated to be approximately 2% for all cases.

The center of mass of the electron assembly, Z_c, the averaged squared radial deviation from the axis, $\langle R^2 \rangle$, and the averaged squared longitudinal deviation from the center of mass, $\langle (Z - Z_c)^2 \rangle$, are also calculated at the end of the time section. The values for the drift velocity, V_d, the transverse diffusion coefficient, D_T, and the longitudinal diffusion coefficient, D_L, are obtained in steady state from the slopes of the least-squares straight line (local) fit of the Z_c, $\langle R^2 \rangle$, and $\langle (Z - Z_c)^2 \rangle$ versus time data, respectively. The volume ionization coefficient, α, is obtained from the slope of the least-squares straight line (local) fit of the Z_c versus n data, where n is the number of electrons in the avalanche. In the region where the growth is exponential, the maximum percentage deviation of the data from the straight line approximation is approximately 1% for 300 Td.

The evolution of some of the rate coefficients and transport parameters are shown in Figs. 4 and 5. Note that in the quasi-steady-state regime (i.e., before the influence of the space-charge field becomes significant), the fluctuation in the above parameter is small. This illustrates the equivalence of the assemblies before and after the mapping.

At the end of a time section, the electrons and ion densities obtained from the Monte Carlo simulation are "smoothed" using a two-dimensional, discrete, Legendre polynomial expansion to least square approximate the densities over a local area (typically an array of 6×6 grid points). The "smoothed" densities are then used as sources in the Poisson equation. This smoothing is only for the purpose of computing the space-charge electric field. The sum of this field and the applied field are then used to update the properties of the electrons in the next time section. The effect of the space-charge field on the evolution of the assembly can also be seen in Figs. 4 and 5. Inside the electron assembly, the space-charge field is opposite to the applied field, so that the total field in this region decreases with time. This causes a decrease in the mean energy with time as shown in Fig. 4. The increase observed in the drift velocity (Fig. 4) is due to the fact that the flow of electrons near the front of the assembly is highly directional (towards the anode). This is caused by the enhanced field at the edges of the assembly. The earliest effect of the space-charge field is observed on the transverse diffusion coefficient. It is never observed to have a region of quasi-steady-state (see Fig. 5). Since the applied radial field is zero, the radial space-charge field immediately influences the transverse evolution of the assembly. Along the applied field direction, however, the effect of the space-charge

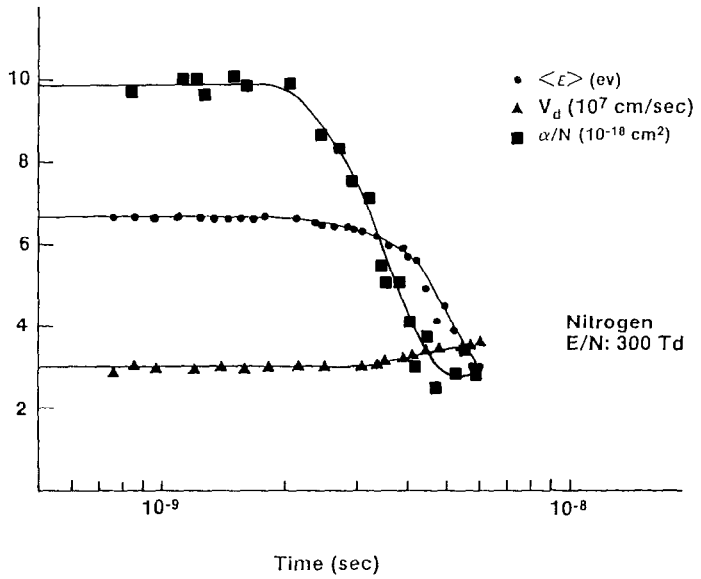

FIG. 4. Evolution of mean energy, $\langle \varepsilon \rangle$, drift velocity V_d, and ionization coefficient α. N is the density of background neutrals.

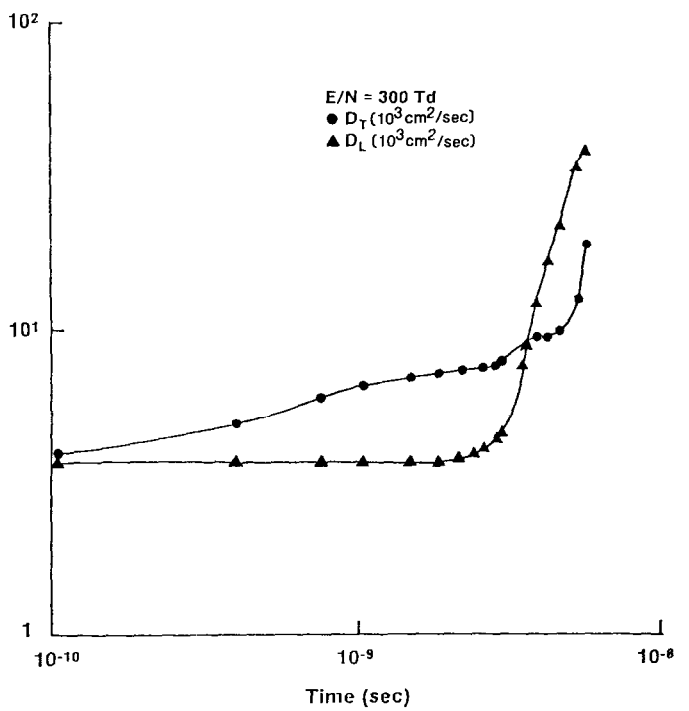

FIG. 5. Evolution of diffusion coefficients.

field on the longitudinal diffusion coefficient (Fig. 5) is not important, until the space-charge field becomes of the order of the applied field. The longitudinal coefficient is nearly constant until this time.

IV. Concluding Remarks

The example given in the previous section illustrates the power of the Monte Carlo technique presented in Section II. With it, it is possible to simulate the behavior of an assembly of particles whose number is increasing with time and whose evolution depends on the total number of particles. This technique is easily implemented. The code we have written (Fig. 2) has been run on VAX–780 minicomputer. The runs for the example discussed in the previous section lasted a few hours.

Acknowledgments

This work was supported in part by the Office of Naval Research and by the Naval Surface Weapons Center.

References

1. T. Wu, *Kinetic Equations of Gases and Plasmas* (Addison–Wesley, Reading, MA, 1966), p. 31.
2. J. P. Price, *IBM J. Res. Develop.* **17**, 39 (1973).
3. C. Jacoboni and L. Reggioni, *Rev. Mod. Phys.* **55**, 645 (1983).
4. R. W. L. Thomas and W. R. L. Thomas, *J. Phys. B: Atom. Phys.* **2**, 562 (1969).
5. J. M. Hammarsley and D. C. Handscomb, *Monte Carlo Methods* (Methuen, London, 1964), p. 50.
6. H. D. Rees, *Phys. Lett., A* **26**, 416 (1968).
7. H. R. Skullerud, *J. Phys. D: Appl. Phys.* **1**, 1567 (1968).
8. W. Fawcett, D. A. Boardman and S. Swain, *J. Phys. Chem. Solids* **31**, 1963 (1970).
9. S. L. Lin and J. N. Bardsley, *Comput. Phys. Commun.* **15**, 161 (1978).
10. T. Kurosawa, *J. Phys. Soc. Japan Suppl.* **21**, 424 (1966).
11. Y. Tzeng and E. E. Kunhardt, *Physical Review A*, to appear.
12. E. E. Kunhardt and Y. Tzeng, in *Proceedings of the Fourth International Symposium on Gaseous Dielectrics, Knoxville, Tenn., 1984*, edited by L. G. Christophoron and M. O. Pace (Pergamon, Elmsford, NY, 1984), p. 146.
13. E. E. Kunhardt and P. F. Williams, *J. Comput. Phys.* **57**, 403 (1985).
14. C. B. Opal, W. K. Peterson, and E. C. Beaty, *J. Chem. Phys.* **55**, 4150 (1971).